

Spin-polarised DFT modeling of electronic, magnetic, thermal and optical properties of silicene doped with transition metals

Nzar Rauf Abdullah^{a,b}, Mohammad T. Kareem^c, Hunar Omar Rashid^a, Andrei Manolescu^d, Vidar Gudmundsson^e

^a*Division of Computational Nanoscience, Physics Department, College of Science, University of Sulaimani, Sulaimani 46001, Kurdistan Region, Iraq*

^b*Computer Engineering Department, College of Engineering, Komar University of Science and Technology, Sulaimani 46001, Kurdistan Region, Iraq*

^c*Chemistry Department, College of Science, University of Sulaimani, Sulaimani 46001, Kurdistan Region, Iraq*

^d*Reykjavik University, School of Science and Engineering, Menntavegur 1, IS-101 Reykjavik, Iceland*

^e*Science Institute, University of Iceland, Dunhaga 3, IS-107 Reykjavik, Iceland*

arXiv:2009.14804v1 [cond-mat.mes-hall] 30 Sep 2020

Abstract

The geometric, electronic, magnetic, thermal, and optical properties of transition metal (TM) doped silicene are systematically explored using spin-dependent density functional computation. We find that the TM atoms decrease the buckling degree of the silicene structure caused by the interaction between the dopant TM atoms and the Si atoms in the silicene layer plane which is quite strong. In some TM-silicenes, parallel bands and the corresponding van Hove singularities are observed in the electronic band structure without and with spin-polarization. These parallel bands are the origin of most of the transitions in the visible and the UV regions. A high Seebeck coefficient is found in some TM-silicene without spin-polarization. In the presence of emergent spin-polarization, a reduction or a magnification of the Seebeck coefficient is seen due to a spin-dependent phase transition. We find that the preferred state is a ferromagnetic state with a very high Curie temperature. We observe a strong interaction and large orbital hybridization between the TM atoms and the silicene. As a result, a high magnetic moment emerges in TM-silicene. Our results are potentially beneficial for thermospin, and optoelectronic nanodevices.

Keywords: Magnetization, Thermal transport, Silicene, DFT, Electronic structure, Optical properties

1. Introduction

A two-dimensional allotrope of silicon is silicene, which was first reported in 1994 [1]. Silicene has a periodically buckled topology leading to different properties compared to some other 2D materials [2, 3], and it is composed of silicon (Si) atoms with some benefits compared to graphene [4, 5] as it is compatible with the present silicon-based technology. Therefore, silicene has been extensively investigated in electronics [6], optical [7], thermoelectric [8], and magnetic [9] devices. Silicenes with Transition metals (TM) have also several applications in chemistry such as hydrogenation evolution reaction [10], designing oxygen reduction reaction electro-catalysts [11], and silicene superlattice for Na-ion [12] Li-O₂ [13] batteries.

Despite its unique properties, silicene is not a very good material for some applications such as thermoelectric devices due to the zero bandgap. However, the zero-gap disadvantage can be overcome [14]. Transition metals (TM) doped silicene (TM-silicene) are candidates in which the bandgap can be tuned [15]. It has been shown that in TM the semi-metal characteristics of silicene are changed to be

semiconducting or metallic depending on the type of the TM dopant atoms. Among the ten types of TM-silicene investigated, Ti-, Ni-, and Zn-doped silicene have shown semiconducting properties, whereas Co- and Cu- doped silicene present a half-metallic material [16].

In addition to the advantage found in the aforementioned studies, another point speaking for TM-silicene is that it is a strong candidate for the quantum spin Hall effect. This is again attributed to the enhanced bandgap of TM-silicene [17, 18]. Therefore, the investigations of the magnetic properties of TM-silicene are of potential importance in diverse fields such as quantum electronics, spintronics, and optoelectronics [17, 19]. It has been shown that the magnetic behavior of silicene can also be tuned by different TM dopant atoms [20]. The magnetic modifications mainly come from the 3d orbitals of the TM dopant atoms along with a partial contribution from the adjacent Si atoms.

The optical properties of silicene is another important aspect of research because it also has many applications in the optoelectronic industries [20, 21]. It has been reported that optical response of silicene is in the IR and visible regions [22]. The absorption spectra of P and Al-doped silicenes show higher absorption compared to pristine silicene, and no important changes in the electrical

Email address: nzar.r.abdullah@gmail.com (Nzar Rauf Abdullah)

conductivity are found with the doping concentration for in-plane light polarization [23]. The optical properties of TM-doped silicene have shown that the intensity of the absorption peaks decreases for out of the plane light polarization [24].

The thermoelectric characteristics of pristine silicene can also be improved by doping. For example, the presence of defects may decrease the phononic thermal conductance. This enhances the thermoelectric efficiency or the figure of merit ZT [25]. A substitutional B/N doping [26] and dihydrogenation [27] of silicene have been regarded as an effective way to enhance the thermoelectric efficiency. All the methods used to increase the thermoelectric efficiency focus on tuning the bandgap of the silicene structure.

In this work, we consider the effects of TM doping on the physical properties of silicene. We first study the electronic, thermal and optical characteristics of TM-silicene. We then use a TM dopant as a prototype magnetic impurity to show that it is possible to achieve magnetic properties such as ferro- or antiferromagnetism. We will show how magnetically active phases in TM-silicene can enhance the thermoelectric properties such as the Seebeck coefficient. It will be shown that TM-doped silicene monolayers could be prominent candidates for spintronic devices.

In Sec. 2 the structure of TM-silicene is briefly overviewed. In Sec. 3 the main achieved results are analyzed. In Sec. 4 the conclusions of the modeling results are presented.

2. Computational Tools

All the calculations of the pure and the TM-silicene properties are performed with the Quantum espresso (QE) simulation package [28, 29]. For visualization of the samples, the crystalline and molecular structure the visualization program (XCrySDen) is used [30]. In QE, the general gradient approximation (GGA) with the Perdew-Burke-Ernzerhof (PBE) potential is employed with a cut-off energy of 1088.45 eV. In our samples consisting of a 2×2 supercell, the structures are considered fully relaxed when the Hellmann-Feynman forces are less than 1.2×10^{-4} eV/Å, and the total energy changes less than 1.9×10^{-4} eV. The Brillouin zone (BZ) is sampled by a Monkhorst-Pack k -mesh of $15 \times 15 \times 1$. The same k -mesh points are used for the SCF calculations. In the density of state (Dos) calculations, a $100 \times 100 \times 1$ grids are used. Furthermore, the Boltzmann transport properties software package (BoltzTraP) is utilized to study the thermal properties of the structures [31]. The BoltzTraP code uses a mesh of band energies and has an interface to the QE package [32]. The optical characteristics of the systems are obtained by the QE code with a broadening of 0.1 eV.

3. Results

Our results are divided into two groups: First, the results of the spin-independent model, the electronic, the

thermal and optical properties for TM-silicene. Second, we show the results of the spin-dependent model, the electronic band structure, the density of states of TM-silicene, and the thermal properties. In addition the magnetic properties including the magnetic moments of TM-silicene are presented.

3.1. Spin-independent calculations

In this section, we show the results of the spin-independent model. The structures under investigation are shown in Fig. 1. The left panel of Fig. 1 is the pristine buckled silicene, b-Si (top panel), and the TM-doped silicene (bottom panel). In addition, the right panel is the side view of the b-Si and TM-silicene for five selected TM dopants including Ti, V, Mn, Fe, and Co atoms. The TM atoms are doped at the para-positions of the 2×2 hexagonal structure of silicene [33, 34, 35]. The TM-silicene is thus identified as TiSi₇ (purple), VSi₇ (red), MnSi₇ (light blue), FeSi₇ (blue), and CoSi₇ (black). In b-Si, the Si-Si bond length is found to be 2.27 Å, which agrees well with a previous study [36]. This larger Si-Si bond length weakens the π - π overlaps, resulting in a low-buckled structure. The buckling parameter of b-Si is 0.45 Å which is in a good agreement with previous studies [37].

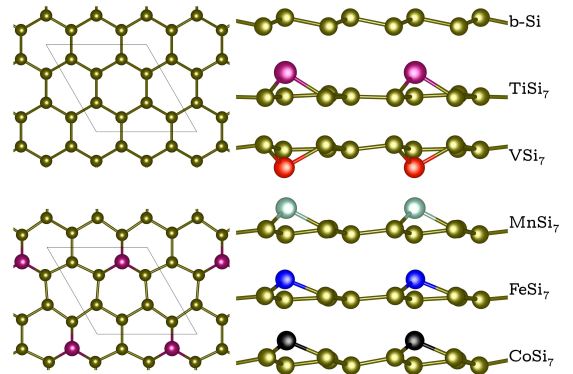


Figure 1: Left panel: the pure silicene, b-Si, (top panel) and the TM-doped silicene (bottom panel). Right panel: side view of b-Si (golden), TiSi₇ (purple), VSi₇ (red), MnSi₇ (light blue), FeSi₇ (blue), and CoSi₇ (black).

Table 1: The buckling parameter of the structures.

Structure	$\delta(\text{Å})$
b-Si	0.45
TiSi ₇	0.076
VSi ₇	0.2
MnSi ₇	0.268
FeSi ₇	0.174
CoSi ₇	0.371

The first observation of Fig. 1 is that the buckling degree is strongly influenced by the TM atom dopant. The buck-

ling parameter (δ) for all structures under investigation are presented in Tab. 1.

It can be seen that the TM atoms leave the silicene plane in the fully relaxed structures [38]. Consequently, the buckling degree of TM-silicene is decreased compared to b-Si. The outward movement of the TM atoms from the silicene layer and the occupation of almost perfectly symmetric 3-fold positions have been reported previously [39]. This reveals that in contrast to graphene the interaction between the TM atoms and the silicene layer is quite strong due to its highly reactive buckled hexagonal structure [40]. The lowest buckling degree occurring for TiSi₇ reveals a maximum distortion, and the highest buckling degree of CoSi₇ among TM-silicene indicates a minimum distortion in the silicene structure. These distortions emerge here because the bonding energy of the Ti atoms, 4.89 eV, to silicene occurs with a significant buckling and lattice a distortion [40]. In addition, the atomic radii of the Ti atoms are much larger than these of the Co atoms which may influence the distortion and the buckling degree.

The DFT calculations of the formation energy indicate that TiSi₇ has the lowest, and CoSi₇ has the highest formation energy among all the investigated structures. The TiSi₇ is thus the most structurally stable system.

The electronic band structures of b-Si (a) and the TM-silicenes (b-f) are presented in Fig. 2. The electronic eigenvalues along high symmetry directions (Γ M K Γ) in the first Brillouin zone are calculated self-consistently. Our results for the band structure show that the TiSi₇ (b) and VSi₇ (c) are semiconducting materials due to the presence of a finite bandgap around Fermi energy, while MnSi₇ (d), FeSi₇ (e), and CoSi₇ (f) are metals because the Fermi energy crosses valence or conduction bands. The bandgap of TiSi₇ and VSi₇ are 0.51 and 0.59 eV, respectively. It should be noticed that the Dirac cone in the TM silicene vanishes. This is caused by the orbitals of the TM atom which make a considerable contribution to the energy levels through the hybridization between the TM atom and the silicene as is seen in Fig. 2(g). It can be clearly seen the density of states of the TM atom around the Fermi energy has a high contribution. The semiconductor properties of some TM-silicenes with Ti dopant atoms have recently been studied [24].

The bandgap tuning directly influences the thermoelectric properties of a system. The Seebeck coefficient, S , of a pristine b-Si and TM-silicenes are displayed in Fig. 3 at temperature $T = 100$ K. We focus on this low temperature range from 20 to 160 K, where the electrons and phonons are decoupled. At this temperature range the electrons deliver the main contribution to the thermal behavior [41, 42, 43]. The gapless b-Si exhibits poorer thermoelectric performance, than the gapped TM-silicenes. The low Seebeck coefficient and the thermoelectric performance of b-Si is caused by the cancellation of the electron-hole contributions to the transport quantities. As we stated before, an effective way to enhance the thermoelectric properties

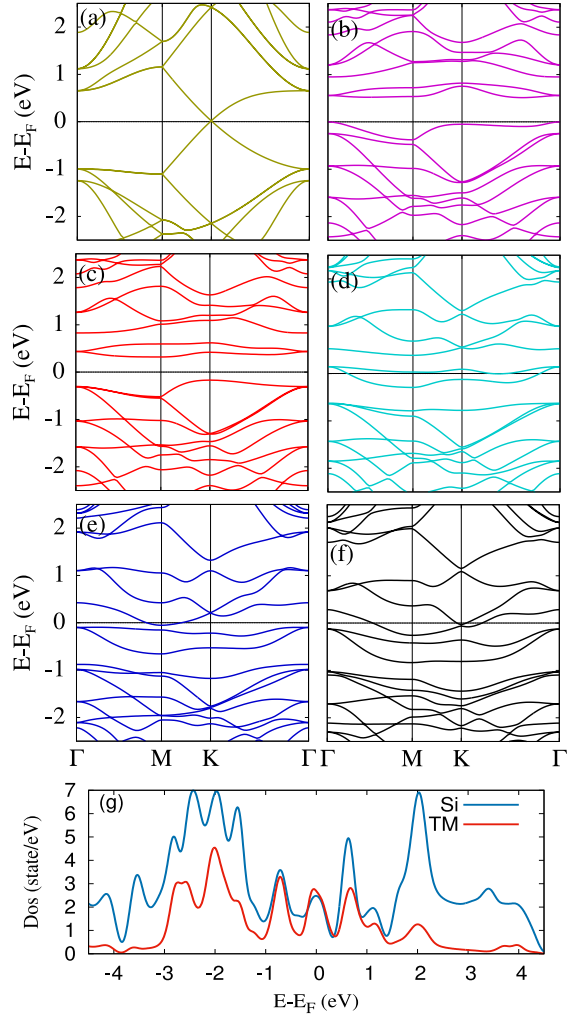


Figure 2: The electronic band structure of b-Si (a), TiSi₇ (b), VSi₇ (c), MnSi₇ (d), FeSi₇ (e), and CoSi₇ (f). The density of state (Dos) of the Si and TM atoms in TM-silicene, FeSi₇, (g). The Fermi energy is set at zero.

of a system is to open up a bandgap, and thus lifting this cancellation effect [44].

We therefore see the maximum Seebeck coefficient for TiSi₇ (purple) and VSi₇ (red) as they have a bandgap around the Fermi energy behaving as semiconductor materials.

The optical response of a 2D structure is also directly related to the electronic band structure [45]. For instance the imaginary part of the dielectric function denotes the absorbed energy by the structure. The imaginary dielectric functions, ϵ_2 , in the case of an in-plane or a parallel, E_{in} , (a) and an out-plane or a perpendicular, E_{out} , (b) electric fields are shown in Fig. 4 for b-Si and TM-silicene. It is well known that the two main peaks in the imaginary dielectric function of b-Si are at 1.68 eV corresponding to the π to π^* states, and at 3.85 eV revealing the transition between the σ to the σ^* states in the parallel electric field. Similar to graphene, inter-band transitions for perpendicular polarized light are observed for pristine b-Si except

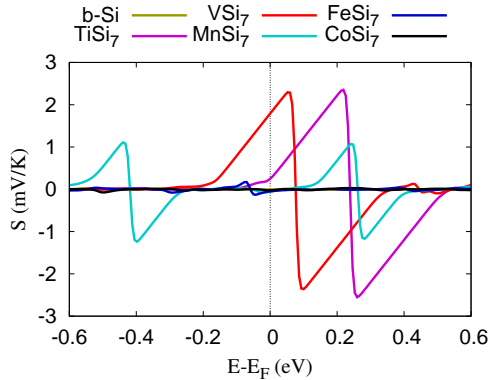


Figure 3: Seebeck coefficient of the b-Si (golden) and the TM-silicene at temperature $T = 100$ K. including TiSi_7 (purple), VSi_7 (red), MnSi_7 (light blue), FeSi_7 (blue), and CoSi_7 (black).

the transitions here occur below 10 eV.

It is interesting to see that the optical response for TM-silicene is strong at low energy (in the visible and the UV regions) for both the parallel and the perpendicular polarizations of the electromagnetic fields. This is attributed to the following facts related to the band structure of TM-silicene. First, the gap at the Γ point in the band structure for all TM-silicene decreases with a increasing atomic radius of the dopant atoms. The higher the atomic radius the smaller gap at Γ point is. Second, parallel bands are formed in all directions between bonding and antibonding orbitals of the TM-silicene. These parallel bands lead to most of the transitions in the visible and the UV regions. Third, optical transitions occur around van Hove singularities. A van Hove singularity is caused by a flat band formed along the M to K as is seen in the band structure of MnSi_7 and CoSi_7 . The effects of a van Hove singularity on the optical response have been reported for 2D materials [22].

3.2. Spin-dependent calculations

In this section, we show the results of a spin-dependent model for the pristine b-Si and the TM-silicenes. First, we preform both ferromagnetic (FM) and antiferromagnetic (AFM) calculations where the strength of the magnetization is assumed to be 0.5 A/m. The energy difference between the AFM and the FM states is $\Delta E = E_{\text{AFM}} - E_{\text{FM}}$. The ΔE of TiSi_7 is zero indicating a nonmagnetic structure, and for VSi_7 , MnSi_7 , FeSi_7 , and CoSi_7 the differences are 85.05, 50.05, 13.6, and -78.9 meV, respectively. This shows that the VSi_7 , MnSi_7 , and FeSi_7 favor FM, but CoSi_7 favors AFM.

Based on ΔE , one can further estimate the Curie temperature, T_C^{MFA} , via a mean field approximation using

$$\frac{3}{2}k_B T_C^{\text{MFA}} = \frac{\Delta E}{N_{\text{imp}}}, \quad (1)$$

with N_{imp} the number of TM atoms in the structure. The Curie temperature of TiSi_7 , VSi_7 , MnSi_7 , FeSi_7 , and CoSi_7

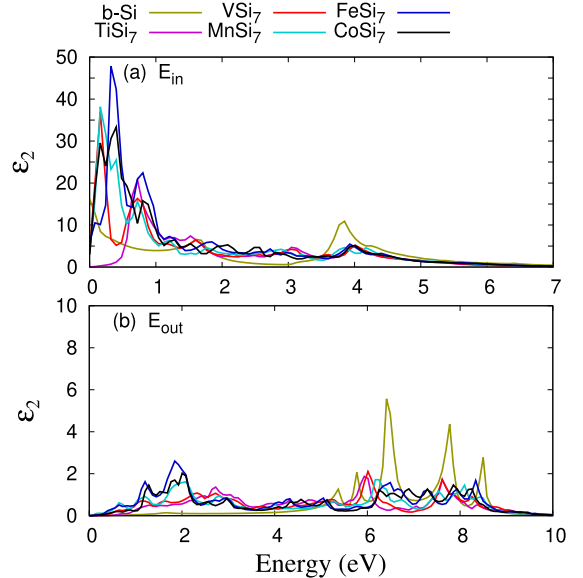


Figure 4: The imaginary dielectric function of pristine b-Si (golden) and TM-silicene including TiSi_7 (purple), VSi_7 (red), MnSi_7 (light blue), FeSi_7 (blue), and CoSi_7 (black) for in-plane, E_{in} , or parallel (a) and out-plane or perpendicular, E_{out} , (b) electric fields.

is found to be 0, 657, 386, 105, and 609 K. The results for the Curie temperatures in our calculations agree well with a previous study [39], and they are candidates for thermospin devices at 100 K as our study shows.

It is known that the TM atoms have a strong coupling with silicene giving a strong modification of the spin-dependent band structures, density of states, and spin transport properties [39]. Figure 5 and 6 show the electronic band structure and the Dos of b-Si and TM-silicene for both spin-up (solid lines) and spin-down (dotted lines), respectively. The band structure and the Dos for b-Si re-

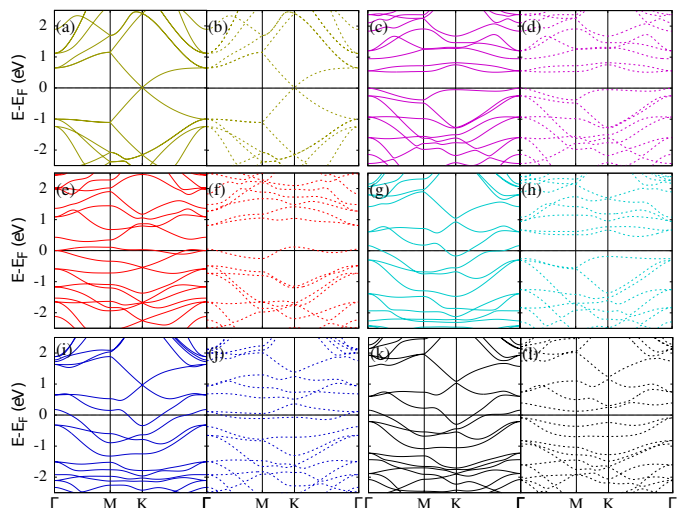


Figure 5: Spin-dependent electronic band structure of b-Si (golden) and TM-silicene including TiSi_7 (purple), VSi_7 (red), MnSi_7 (light blue), FeSi_7 (blue), and CoSi_7 (black). The solid lines are spin-up and dotted lines are spin-down. The Fermi energy is at 0.

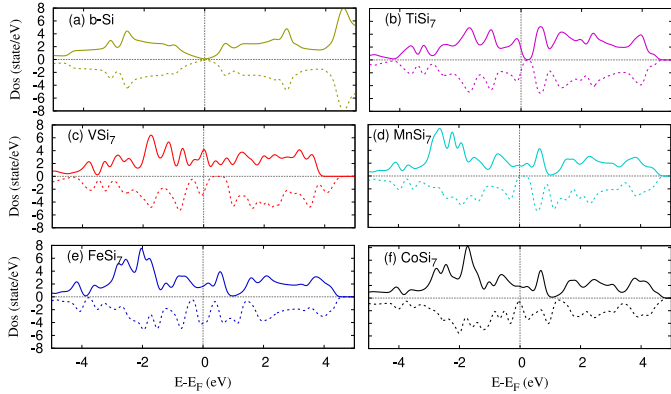


Figure 6: Spin-dependent Dos of b-Si (golden) and TM-silicene including TiSi₇ (purple), VSi₇ (red), MnSi₇ (light blue), FeSi₇ (blue), and CoSi₇ (black). The solid lines are spin-up and dotted lines are spin-down. The Fermi energy is at 0.

veals that the spin-up and the spin-down band structures and Dos are symmetric indicating no magnetic properties. In addition, a spin splitting does not occur between the spin-up and the spin-down close to the Fermi energy showing the pristine b-Si is non-magnetic.

In the TM-silicene, the band structures and the Dos manifest different trends such as nonmagnetic semiconductors, magnetic metals, and half-metals. Namely, TiSi₇ (purple) has nonmagnetic or spin unpolarized semiconducting property with bandgap 0.51 eV for both spin channels. The bandgap here is exactly equal to the bandgap of the structure predicted by the spin-independent model mentioned before. Spin unpolarized semiconducting is a semiconductors having a bandgap but there is no spin splitting between the spin-up and spin-down, and both spin channels have the same structure. These structures are called nonmagnetic semiconductors. Furthermore, VSi₇ (red) and FeSi₇ (blue) indicate a magnetic or spin polarized metallic behavior with a spin splitting between the spin-up and the spin-down states around the Fermi energy, and the Fermi energy crosses the valence or the conduction bands. In the two TM-silicene, MnSi₇ (light blue) and CoSi₇ (black), we notice a spin polarized half-metallic feature with the states of one spin direction showing a semiconducting behavior, while the other displays a metallic behavior. Such property is a basis for spintronic applications. The indirect bandgap of the spin-down channel of MnSi₇ is 0.64 eV, and CoSi₇ it is 0.21 eV. It is interesting to see that VSi₇ has a semiconductor property, when the spin is ignored as is shown in Fig. 2c, but in the spin-dependent model VSi₇ becomes metallic. The same applies to MnSi₇ and CoSi₇, which are metallic according to the spin-independent model, but they become half metallic when spin is accounted for. These spin phase transitions have been observed for silicene materials and superlattices [46]. The spin-phase transition process leads to an increase in thermal efficiency. For instance, the spin-independent Seebeck coefficient of MnSi₇ and CoSi₇ were small shown in Fig. 3, but the spin-polarized Seebeck coef-

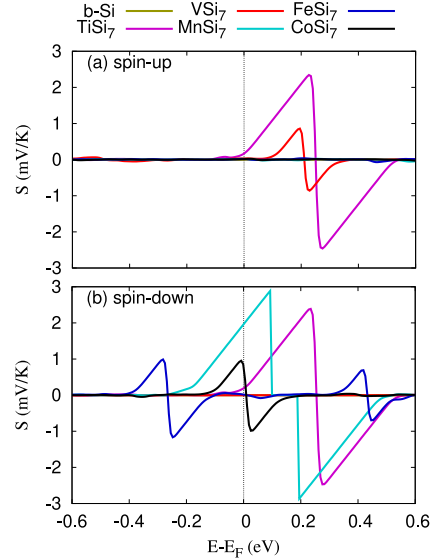


Figure 7: Seebeck coefficient of b-Si and TM-silicene at $T = 100$ K for both spin-up (a) and spin-down (b) channels.

ficient of MnSi₇ and CoSi₇ is enhanced for the spin-down channel as is shown in Fig. 7. This is attributed to the opening of bandgaps for the spin-down channel making them half-metals. It should be mentioned that the Seebeck coefficient of TiSi₇ is the same for both spin-up and down because TiSi₇ is nonmagnetic material. In contrast, the spin-independent Seebeck coefficient of VSi₇ was high but it is suppressed for spin-up and totally vanished for spin-down channel. This spin-dependent phase transition is an important property, through which a bandgap can be induced by means of magnetic dopants. The systems with such a bandgap can be applicable to practical areas, such as field-effect transistors (FETs) [2], single-spin electron sources [47], and nonvolatile magnetic random access memory [48]. This is also important for thermospin filtering in spintronic devices.

The spin-dependent phase transition can mainly be referred to the spin-dependent orbitals of the TM atoms, which contribute to the energy level through the hybridization between the TM atom and the silicene layer as is presented in Fig. 8. We clearly see that the density of state of the TM atom for both spin-up and spin-down around the Fermi energy has high contributions. Especially, the spin-down density of states of TM atoms is much stronger around the Fermi energy compared to the spin-up states.

Another magnetic property of the TM-silicene is the magnetic moment. The 3d-orbitals of the TM atoms gives rise to the magnetism of TM-silicene, and its partial density of state difference for both spin-up and spin-down states shown in Fig. 9, which is responsible for the net magnetic moment. In particular, one can observe that the PDos (partial Dos) peaks of the d-orbitals of the transition metal, d-TM, can align with the peaks of the p-orbitals of the Si atoms of silicene, p-Si, very well. This implies that there are the strong interaction and large orbital hybridiza-

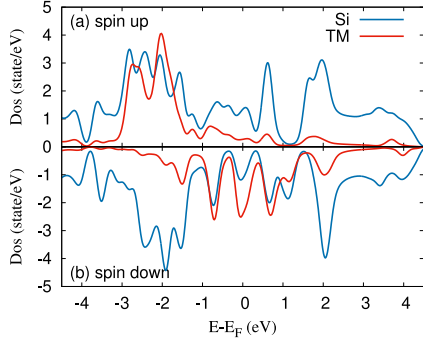


Figure 8: The spin-dependent density of state of the Si and TM atoms in TM-silicene, FeSi₇, for spin-up (a) and spin-down (b).

tion between the TM atoms and the silicene. As a result, high magnetic moments are found in TM-silicene.

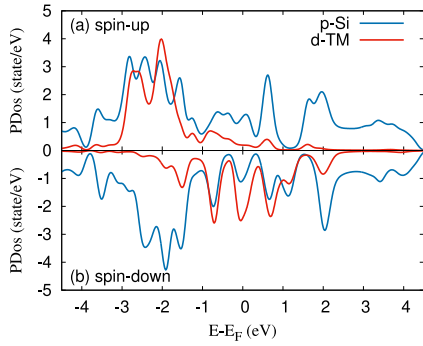


Figure 9: The partial density of state, PDos, of the d-orbital of TM-atom, d-TM, and p-orbital of Si atoms of silicene, p-Si, for both spin-up (a), and spin-down (b).

Figure 10 shows the magnetic moments of the b-Si and the TM-silicene systems for the p-orbital contribution of the Si atoms (μ_p), 3d orbitals of the TM atoms (μ_{3d}), and the total magnetization of the TM-silicene (μ_{Total}). One can clearly see that the magnetization is mainly caused by the TM atoms. In addition, we should remember that our results for the magnetic moment is underestimated by the GGA-PBE calculations. If GGA+U or HSE calculations are used, the obtained magnetic moments will be higher. For instance, the magnetic moment of MnSi₇ is $3\mu_B$ using the GGA-PBE approach, but it is increased to $4\mu_B$ if the GGA+U or HSE are used. This smaller value of magnetic moment of MnSi₇ here can be attributed to the fact that, the semilocal GGA functional tends to delocalize the *d* electrons and increase the *d-p* overlapping, consequently leading to the underestimation of the magnetic moment of the Mn dopant [39].

In order to give a more clear picture of the magnetic distribution, we plot the spin polarized density ($\Delta\rho = \rho_{up} - \rho_{down}$) in Fig. 11 for b-Si and TM-silicene. The spin polarized distribution of b-Si and TiSi₇ is very small. It is neglectable even on the finer scale used on these two subfigures (see the scale of the z-axis). Remarkably, The spin polarized distribution of other TM-silicenes is almost

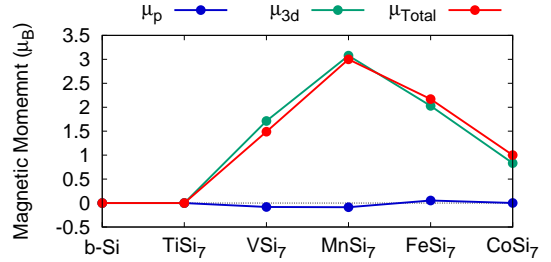


Figure 10: Magnetic moments of b-Si and TM-silicene for the p-orbital contribution of Si atoms (μ_p), 3d orbitals of TM atoms (μ_{3d}), and total magnetization of TM-silicene (μ_{Total}).

entirely located on the dopant atoms, showing highly localized magnetic features. Especially, the spin polarization of the Mn atom in MnSi₇ is highest, revealing the highest magnetic moment as was mentioned before.

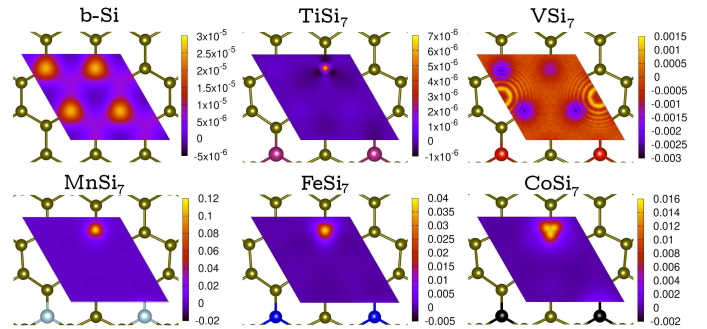


Figure 11: The spin polarized density of b-Si and TM-silicene structures.

4. Summary and Conclusions

We have studied TM-silicene with density functional computation models neglecting, or accounting for spin-polarization. In the absence of spin-polarization in TM-silicene, we observe both metallic and semiconductor behavior depending on the TM dopant atoms. As a result a thermoelectric property such as the Seebeck coefficient is enhanced, and TM-silicenes show a large optical response at low energy. In the presence of spin-polarization in TM-silicene, a spin phase transitions occurs leading to half metallic, metallic, and semiconductor properties of the TM-silicene. The spin phase transitions induce spin filtering or the possibility to access a thermospin transport via spin-up and down channels depending on the spin-dependent band structure. In addition, strong orbital interactions between the Silicon and the TM atoms are observed. These interactions control the magnetization of the system, in which a high magnetic moment of TM-silicene is generated.

5. Acknowledgment

This work was financially supported by the University of Sulaimani and the Research center of Komar University of Science and Technology. The computations were performed on resources provided by the Division of Computational Nanoscience at the University of Sulaimani.

References

- [1] K. Takeda and K. Shiraishi, "Theoretical possibility of stage corrugation in si and ge analogs of graphite," *Phys. Rev. B*, vol. 50, pp. 14916–14922, Nov 1994. [Online]. Available: <https://link.aps.org/doi/10.1103/PhysRevB.50.14916>
- [2] L. Tao, E. Cinquanta, D. Chiappe, C. Grazianetti, M. Fanciulli, M. Dubey, A. Molle, and D. Akinwande, "Silicene field-effect transistors operating at room temperature," *Nature Nanotechnology*, vol. 10, no. 3, pp. 227–231, Mar 2015. [Online]. Available: <https://doi.org/10.1038/nnano.2014.325>
- [3] T.-T. Jia, X.-Y. Fan, M.-M. Zheng, and G. Chen, "Silicene nanomeshes: bandgap opening by bond symmetry breaking and uniaxial strain," *Scientific Reports*, vol. 6, no. 1, p. 20971, Feb 2016. [Online]. Available: <https://doi.org/10.1038/srep20971>
- [4] J. Zhao, H. Liu, Z. Yu, R. Quhe, S. Zhou, Y. Wang, C. C. Liu, H. Zhong, N. Han, J. Lu, Y. Yao, and K. Wu, "Rise of silicene: A competitive 2d material," *Progress in Materials Science*, vol. 83, pp. 24 – 151, 2016. [Online]. Available: <http://www.sciencedirect.com/science/article/pii/S0079642516300068>
- [5] H. O. Rashid, N. R. Abdullah, and V. Gudmundsson, "Silicon on a graphene nanosheet with triangle- and dot-shape: Electronic structure, specific heat, and thermal conductivity from first-principle calculations," *Results in Physics*, vol. 15, p. 102625, 2019. [Online]. Available: <http://www.sciencedirect.com/science/article/pii/S2211379719317140>
- [6] G. Le Lay, "Silicene transistors," *Nature Nanotechnology*, vol. 10, no. 3, pp. 202–203, Mar 2015. [Online]. Available: <https://doi.org/10.1038/nnano.2015.10>
- [7] T.-N. Do, G. Gumbs, P.-H. Shih, D. Huang, C.-W. Chiu, C.-Y. Chen, and M.-F. Lin, "Peculiar optical properties of bilayer silicene under the influence of external electric and magnetic fields," *Scientific Reports*, vol. 9, no. 1, p. 624, Jan 2019. [Online]. Available: <https://doi.org/10.1038/s41598-018-36547-1>
- [8] H.-H. Fu, D.-D. Wu, Z.-Q. Zhang, and L. Gu, "Spin-dependent seebeck effect, thermal colossal magnetoresistance and negative differential thermoelectric resistance in zigzag silicene nanoribbon heterojunction," *Scientific Reports*, vol. 5, no. 1, p. 10547, May 2015. [Online]. Available: <https://doi.org/10.1038/srep10547>
- [9] A. M. Tokmachev, D. V. Averyanov, O. E. Parfenov, A. N. Taldenkov, I. A. Karateev, I. S. Sokolov, O. A. Kondratev, and V. G. Storchak, "Emerging two-dimensional ferromagnetism in silicene materials," *Nature Communications*, vol. 9, no. 1, p. 1672, Apr 2018. [Online]. Available: <https://doi.org/10.1038/s41467-018-04012-2>
- [10] Y. Sun, A. Huang, and Z. Wang, "Transition metal atom (ti, v, mn, fe, and co) anchored silicene for hydrogen evolution reaction," *RSC Adv.*, vol. 9, pp. 26321–26326, 2019. [Online]. Available: <http://dx.doi.org/10.1039/C9RA04602J>
- [11] H. Dong, Y. Ji, L. Ding, and Y. Li, "Strategies for computational design and discovery of two-dimensional transition-metal-free materials for electro-catalysis applications," *Phys. Chem. Chem. Phys.*, vol. 21, pp. 25535–25547, 2019. [Online]. Available: <http://dx.doi.org/10.1039/C9CP04284A>
- [12] J. Zhu and U. Schwingenschlgl, "Silicene for nanion battery applications," *2D Materials*, vol. 3, no. 3, p. 035012, aug 2016. [Online]. Available: <https://doi.org/10.1088%2F2053-1583%2F3%2F3%2F035012>
- [13] W. Zhang, L. Sun, J. M. V. Nsanzimana, and X. Wang, "Lithiation/delithiation synthesis of few layer silicene nanosheets for rechargeable li-o₂ batteries," *Advanced Materials*, vol. 30, no. 15, p. 1705523, 2018.
- [14] H. Sadeghi, S. Sangtarash, and C. J. Lambert, "Enhanced thermoelectric efficiency of porous silicene nanoribbons," *Scientific Reports*, vol. 5, no. 1, p. 9514, Mar 2015. [Online]. Available: <https://doi.org/10.1038/srep09514>
- [15] J. Zhang, B. Zhao, and Z. Yang, "Abundant topological states in silicene with transition metal adatoms," *Phys. Rev. B*, vol. 88, p. 165422, Oct 2013. [Online]. Available: <https://link.aps.org/doi/10.1103/PhysRevB.88.165422>
- [16] Y. Lee, K.-H. Yun, S. B. Cho, and Y.-C. Chung, "Electronic properties of transition-metal-decorated silicene," *ChemPhysChem*, vol. 15, no. 18, pp. 4095–4099, 2014. [Online]. Available: <https://chemistry-europe.onlinelibrary.wiley.com/doi/abs/10.1002/cphc.201401002>
- [17] X.-L. Zhang, L.-F. Liu, and W.-M. Liu, "Quantum anomalous hall effect and tunable topological states in 3d transition metals doped silicene," *Scientific Reports*, vol. 3, no. 1, p. 2908, Oct 2013. [Online]. Available: <https://doi.org/10.1038/srep02908>
- [18] C.-C. Liu, W. Feng, and Y. Yao, "Quantum spin hall effect in silicene and two-dimensional germanium," *Phys. Rev. Lett.*, vol. 107, p. 076802, Aug 2011. [Online]. Available: <https://link.aps.org/doi/10.1103/PhysRevLett.107.076802>
- [19] S. A. Wolf, D. D. Awschalom, R. A. Buhrman, J. M. Daughton, S. von Molnár, M. L. Roukes, A. Y. Chtchelkanova, and D. M. Treger, "Spintronics: A spin-based electronics vision for the future," *Science*, vol. 294, no. 5546, pp. 1488–1495, 2001. [Online]. Available: <https://science.sciencemag.org/content/294/5546/1488>
- [20] X. Sun, L. Wang, H. Lin, T. Hou, and Y. Li, "Induce magnetism into silicene by embedding transition-metal atoms," *Applied Physics Letters*, vol. 106, no. 22, p. 222401, 2015. [Online]. Available: <https://doi.org/10.1063/1.4921699>
- [21] N. R. Abdullah, C.-S. Tang, A. Manolescu, and V. Gudmundsson, "The interplay of electron-photon and cavity-environment coupling on the electron transport through a quantum dot system," *Physica E: Low-dimensional Systems and Nanostructures*, vol. 119, p. 113996, 2020. [Online]. Available: <http://www.sciencedirect.com/science/article/pii/S1386947719312445>
- [22] R. John and B. Merlin, "Optical properties of graphene, silicene, germanene, and stanene from ir to far uv a first principles study," *Journal of Physics and Chemistry of Solids*, vol. 110, pp. 307 – 315, 2017. [Online]. Available: <http://www.sciencedirect.com/science/article/pii/S0022369717300367>
- [23] R. Das, S. Chowdhury, A. Majumdar, and D. Jana, "Optical properties of p and al doped silicene: a first principles study," *RSC Adv.*, vol. 5, pp. 41–50, 2015. [Online]. Available: <http://dx.doi.org/10.1039/C4RA07976K>
- [24] Z. H. T. Gheshlagh, J. Beheshtian, and S. Mansouri, "The electronic and optical properties of 3d transition metals doped silicene sheet: A DFT study," *Materials Research Express*, vol. 6, no. 12, p. 126326, jan 2020. [Online]. Available: <https://doi.org/10.1088%2F2053-1591%2F6%2F12%2F126326>
- [25] W. Zhao, Z. Guo, Y. Zhang, J. Ding, and X. Zheng, "Enhanced thermoelectric performance of defected silicene nanoribbons," *Solid State Communications*, vol. 227, pp. 1 – 8, 2016. [Online]. Available: <http://www.sciencedirect.com/science/article/pii/S0038109815004056>
- [26] N. R. Abdullah, H. O. Rashid, C.-S. Tang, A. Manolescu, and V. Gudmundsson, "Properties of bsi₁₋₆n monolayers derived by first-principle computation," *arXiv preprint arXiv:2008.03782*, 2020.
- [27] K. Zborecki, R. Swirkowicz, M. Wierzbicki, and J. Barna, "Enhanced thermoelectric efficiency in ferromagnetic silicene nanoribbons terminated with hydrogen atoms," *Phys. Chem. Chem. Phys.*, vol. 16, pp. 12900–12908, 2014. [Online]. Available: <http://dx.doi.org/10.1039/C4CP01039F>
- [28] P. Giannozzi, S. Baroni, N. Bonini, M. Calandra, R. Car, C. Cavazzoni, D. Ceresoli, G. L. Chiarotti, M. Cococcioni, I. Dabo, A. D. Corso, S. de Gironcoli, S. Fabris, G. Fratesi, R. Gebauer, U. Gerstmann, C. Gougoussis, A. Kokalj,

- M. Lazzeri, L. Martin-Samos, N. Marzari, F. Mauri, R. Mazzeo, S. Paolini, A. Pasquarello, L. Paulatto, C. Sbraccia, S. Scandolo, G. Sciauero, A. P. Seitsonen, A. Smogunov, P. Umari, and R. M. Wentzcovitch, "QUANTUM ESPRESSO: a modular and open-source software project for quantum simulations of materials," *Journal of Physics: Condensed Matter*, vol. 21, no. 39, p. 395502, sep 2009. [Online]. Available: <https://doi.org/10.1088%2F0953-8984%2F21%2F39%2F395502>
- [29] P. Giannozzi, O. Andreussi, T. Brumme, O. Bunau, M. B. Nardelli, M. Calandra, R. Car, C. Cavazzoni, D. Ceresoli, M. Cococcioni *et al.*, "Advanced capabilities for materials modelling with quantum espresso," *Journal of Physics: Condensed Matter*, vol. 29, no. 46, p. 465901, 2017.
- [30] A. Kokalj, "Xcrysden—a new program for displaying crystalline structures and electron densities," *Journal of Molecular Graphics and Modelling*, vol. 17, no. 3, pp. 176–179, 1999. [Online]. Available: <http://www.sciencedirect.com/science/article/pii/S1093326399000285>
- [31] G. K. Madsen and D. J. Singh, "Boltztrap. a code for calculating band-structure dependent quantities," *Computer Physics Communications*, vol. 175, no. 1, pp. 67–71, 2006.
- [32] N. R. Abdullah, G. A. Mohammed, H. O. Rashid, and V. Gudmundsson, "Electronic, thermal, and optical properties of graphene like six structures: Significant effects of si atom configurations," *Physics Letters A*, vol. 384, no. 24, p. 126578, 2020. [Online]. Available: <http://www.sciencedirect.com/science/article/pii/S037596012030445X>
- [33] N. R. Abdullah, H. O. Rashid, M. T. Kareem, C.-S. Tang, A. Manolescu, and V. Gudmundsson, "Effects of bonded and non-bonded b/n codoping of graphene on its stability, interaction energy, electronic structure, and power factor," *Physics Letters A*, vol. 384, no. 12, p. 126350, 2020. [Online]. Available: <http://www.sciencedirect.com/science/article/pii/S0375960120301602>
- [34] N. R. Abdullah, H. O. Rashid, C.-S. Tang, A. Manolescu, and V. Gudmundsson, "Modeling electronic, mechanical, optical and thermal properties of graphene-like bc6n materials: Role of prominent bn-bonds," *Physics Letters A*, vol. 384, no. 32, p. 126807, 2020. [Online]. Available: <http://www.sciencedirect.com/science/article/pii/S0375960120306745>
- [35] N. R. Abdullah, D. A. Abdalla, T. Y. Ahmed, S. W. Abdulqadr, and H. O. Rashid, "Effect of bn dimers on the stability, electronic, and thermal properties of monolayer graphene," *Results in Physics*, vol. 18, p. 103282, 2020. [Online]. Available: <http://www.sciencedirect.com/science/article/pii/S2211379720317496>
- [36] S. Lebègue and O. Eriksson, "Electronic structure of two-dimensional crystals from ab initio theory," *Phys. Rev. B*, vol. 79, p. 115409, Mar 2009. [Online]. Available: <https://link.aps.org/doi/10.1103/PhysRevB.79.115409>
- [37] S. Cahangirov, M. Topsakal, E. Aktürk, H. Şahin, and S. Ciraci, "Two- and one-dimensional honeycomb structures of silicon and germanium," *Phys. Rev. Lett.*, vol. 102, p. 236804, Jun 2009. [Online]. Available: <https://link.aps.org/doi/10.1103/PhysRevLett.102.236804>
- [38] N. R. Abdullah, H. O. Rashid, A. Manolescu, and V. Gudmundsson, "Interlayer interaction controlling the properties of ab-and aa-stacked bilayer graphene-like bc_n and si₂c₁₄," *arXiv preprint arXiv:2008.10888*, 2020.
- [39] S. Li, Z. Ao, J. Zhu, J. Ren, J. Yi, G. Wang, and W. Liu, "Strain controlled ferromagnetic-antiferromagnetic transformation in mn-doped silicene for information transformation devices," *The Journal of Physical Chemistry Letters*, vol. 8, no. 7, pp. 1484–1488, 2017, pMID: 28301928. [Online]. Available: <https://doi.org/10.1021/acs.jpcllett.7b00115>
- [40] H. Şahin and F. M. Peeters, "Adsorption of alkali, alkaline-earth, and 3d transition metal atoms on silicene," *Phys. Rev. B*, vol. 87, p. 085423, Feb 2013. [Online]. Available: <https://link.aps.org/doi/10.1103/PhysRevB.87.085423>
- [41] S. Yiğen, V. Tayari, J. O. Island, J. M. Porter, and A. R. Champagne, "Electronic thermal conductivity measurements in intrinsic graphene," *Phys. Rev. B*, vol. 87, p. 241411, Jun 2013. [Online]. Available: <https://link.aps.org/doi/10.1103/PhysRevB.87.241411>
- [42] N. R. Abdullah, C.-S. Tang, A. Manolescu, and V. Gudmundsson, "Manifestation of the purcell effect in current transport through a dot-cavity-qed system," *Nanomaterials*, vol. 9, no. 7, p. 1023, 2019.
- [43] —, "Thermoelectric inversion in a resonant quantum dot-cavity system in the steady-state regime," *Nanomaterials*, vol. 9, no. 5, p. 741, 2019.
- [44] E. H. Hasdeo, L. P. A. Krisna, M. Y. Hanna, B. E. Gunara, N. T. Hung, and A. R. T. Nugraha, "Optimal band gap for improved thermoelectric performance of two-dimensional dirac materials," *Journal of Applied Physics*, vol. 126, no. 3, p. 035109, 2019. [Online]. Available: <https://doi.org/10.1063/1.5100985>
- [45] N. R. Abdullah, "Rabi-resonant and intraband transitions in a multilevel quantum dot system controlled by the cavity-photon reservoir and the electron-photon coupling," *Results in Physics*, vol. 15, p. 102686, 2019. [Online]. Available: <http://www.sciencedirect.com/science/article/pii/S221137971932251X>
- [46] F. Khoeini and Z. Jafarkhani, "Tunable spin transport and quantum phase transitions in silicene materials and superlattices," *Journal of Materials Science*, vol. 54, no. 23, pp. 14483–14494, Dec 2019. [Online]. Available: <https://doi.org/10.1007/s10853-019-03928-4>
- [47] W.-F. Tsai, C.-Y. Huang, T.-R. Chang, H. Lin, H.-T. Jeng, and A. Bansil, "Gated silicene as a tunable source of nearly 100% spin-polarized electrons," *Nature Communications*, vol. 4, no. 1, p. 1500, Feb 2013. [Online]. Available: <https://doi.org/10.1038/ncomms2525>
- [48] E. C. Ahn, H.-S. P. Wong, and E. Pop, "Carbon nanomaterials for non-volatile memories," *Nature Reviews Materials*, vol. 3, no. 3, p. 18009, Mar 2018. [Online]. Available: <https://doi.org/10.1038/natrevmats.2018.9>